

**Original Research**

## Melatonin, bakuchiol and ascorbyl tetraispalmitate synergize to modulate gene expression and restore Hypoxia-Inducible Factor 1 signaling in UV-exposed skin

Mridvika Narda<sup>1</sup>, Anthony Brown<sup>2</sup>, Daniel Pérez-Cremades<sup>3</sup>, José Luís García-Giménez<sup>3</sup>, Corinne Granger<sup>1\*</sup><sup>1</sup>Innovation and Development, ISDIN, Barcelona, Spain<sup>2</sup>External consultant to ISDIN<sup>3</sup>EpiDisease S.L. (Spin-Off CIBER-ISCIII), Parc Científic de la Universitat de València, Paterna, Spain\*Correspondence to: [mridvika.narda@isdin.com](mailto:mridvika.narda@isdin.com)

Received November 25, 2019; Accepted December 26, 2019; Published December 31, 2019

Doi: <http://dx.doi.org/10.14715/cmb/2019.65.8.7>

Copyright: © 2019 by the C.M.B. Association. All rights reserved.

**Abstract:** Chronic exposure to solar ultraviolet (UV) radiation induces changes to the expression of hundreds of genes in the skin and modulates cellular signaling pathways that alter its structure, function and appearance. To counter these effects, we have developed a 3-in-1 night facial serum (3-in-1 NFS) comprising melatonin, bakuchiol and ascorbyl tetraispalmitate that is designed to attenuate UV-generated free radicals and support new collagen synthesis. In order to better define its mechanism of action and gain insight into how it might influence the biology of photoaged skin, we performed a transcriptomic analysis of *ex vivo* skin explants that had been exposed to UV light and treated with 3-in-1 NFS each day for 4 consecutive days. Differentially expressed mRNAs and microRNAs (miRNA) were identified by RNA sequencing and a miRNA interactome was developed. Pathway enrichment analysis was performed to identify pathways likely modulated by 3-in-1 NFS. Our analysis revealed that the combination of active ingredients in 3-in-1 NFS exerted a synergistic effect on skin biology and modulated the expression of genes implicated in the regulation of collagen biosynthesis, angiogenesis, skin barrier function and cellular metabolism. Pathway analysis indicated that these events are driven by Hypoxia-Inducible Factor 1 $\alpha$  (HIF-1 $\alpha$ ) whose expression in UV-exposed skin was partially restored upon 3-in-1 NFS treatment. To our knowledge, 3-in-1 NFS is the first non-drug demonstrated to act upon this pathway in the skin.

**Key words:** photoaging, ascorbyl tetraispalmitate, melatonin, bakuchiol, skin aging, antioxidant, polyphenol, ultraviolet, HIF-1.

### Introduction

With age, skin gradually loses its structural and morphological integrity and its function begins to decline. This chronic deterioration is enhanced by the cumulative action of various chemical, environmental and mechanical insults. Solar ultraviolet (UV) radiation is especially detrimental, causing skin to lose its elasticity and become deeply wrinkled and leathery in appearance (1). These changes are principally driven by UV-generated reactive oxygen species (ROS) that overwhelm skin's natural antioxidant defense mechanisms and cause damage to cellular proteins, lipids and DNA (1).

Since photoaging is principally the result of oxidative damage by ROS, antioxidants have formed the cornerstone of anti-photoaging treatments and numerous antioxidants and phytochemicals have been tested for their ability to limit or prevent ROS-induced damage. When two or more antioxidants with different mechanisms of actions are combined, antioxidants can synergize and produce better antioxidant activity than the sum of the antioxidants in isolation (2). To this end, we have developed a night facial serum (3-in-1 NFS) designed to prevent and repair the damaging effects of UVR. 3-in-1 NFS combines a direct free radical scavenger (the stable vitamin C derivative ascorbyl tetraispalmitate) (3,4) with an indirect antioxidant that stimulates antioxidative gene expression (melatonin [5-Acetyl-

5-methoxytryptamine]) (5,6), and a phytophenol (bakuchiol [4-[(1E,3S)-3-Ethenyl-3,7-dimethyl-1,6-octadien-1-yl]phenol]) that not only possesses direct and indirect antioxidant activity (7–9) but possesses retinol-like activity and induces collagen expression (7).

In clinical studies 3-in-1 NFS proved to be well-tolerated and reduced facial skin wrinkles and improved its barrier properties (10). Therefore, in an effort to identify its mechanism of action and better understand how it positively impacts skin biology, we performed a global transcriptomic profiling of UV-exposed human skin explants following the application of 3-in-1 NFS.

### Materials and Methods

#### Human *ex vivo* skin explants

Two abdominal skin explants (NativeSkin®), generated from the same donor (healthy Caucasian female, 32 years of age, Fitzpatrick Type II), were purchased from Genoskin (Toulouse, France). Donor skin had not been exposed to sun radiation for at least 2 months prior to harvesting. Explants were placed in 6-well culture plates containing Dedicated Culture Medium (Genoskin, Toulouse, France) and maintained at 37°C, 5% CO<sub>2</sub>, 95% humidity.

#### UV exposure

Skin explants were irradiated at 12.5 J/cm<sup>2</sup> UVA and

50 mJ/cm<sup>2</sup> UVB each day for 4 consecutive days using an Actinic BL TL-K 40W/10-R UVA lamp (Philips, Amsterdam, Netherlands) and UV-B Narrowband PL-L/PL-S lamp (Philips, Amsterdam, Netherlands). Time of exposure, UV dose and UV spectrum had been established previously. After 4 consecutive days, untreated skin exposed to a cumulative dose of 50 J/cm<sup>2</sup> UVA and 200 mJ/cm<sup>2</sup> UVB presented with clear epidermal and dermal alterations (sunburn cell formation, epidermal thickening, melanin accumulation, dermal-epidermal junction flattening and collagen fragmentation) with no loss of viability (data not shown).

### Anti-aging treatment

Treatment groups included 3-in-1 NFS and each of its components (vehicle, melatonin, bakuchiol and ATIP). Melatonin, bakuchiol and ATIP were used at the same concentrations as those in 3-in-1 NFS and in the same vehicle (vehicle composition: Caprylic/Capric Triglyceride, Dicaprylyl Carbonate, Squalane, Alcohol Denat., Caprylyl Glycol, 1,2-Hexanediol, PEG-8; Aqua, Tocopherol, Ascorbyl Palmitate, Citric Acid, Ascorbic Acid).

Briefly, 10 µl of each test item was applied to the surface of NativeSkin® units 1h after irradiation on 4 consecutive days. Before each application, a cotton swab was used to remove the previous day's treatment and the surface of the explant washed twice with PBS. Following the fourth UV-treatment cycle, formulations were left on the surface of the skin for 2 hours before the skin was removed from the matrix and the samples fixed in formalin or frozen in liquid nitrogen.

### RNA extraction

Total RNA was extracted using the *mirVana*<sup>TM</sup> miRNA isolation kit (Invitrogen, Grand Island, NY) according to the manufacturer's instructions. RIN values >9.5 were deemed acceptable for subsequent analysis.

### RNA library preparation

RNA libraries were generated using TruSeq® Stranded mRNA Sample Preparation Kit (Illumina, San Diego, CA) according to the manufacturer's instructions. cDNA libraries were prepared from 1 µg total RNA using TruSeq Stranded mRNA (Illumina, San Diego, CA) and TruSeq RNA Single Indexes Set A (Illumina, San Diego, CA) according to the manufacturer's instructions.

### Small-RNA library preparation

Small-RNA libraries were prepared using the NEXT-FLEX® Small RNA-Seq kit v3 for Illumina Platforms (Bioo Scientific, Austin, TX) following the manufacturer's protocol. Size selection was performed using the Sage Pippin Prep System (Sage Science, Beverly, MA) and 3% Agarose Gel Cassettes (Sage Science, Beverly, MA).

### Sequencing

RNA and small-RNA libraries were sequenced on an Illumina NextSeq 550 (Illumina, San Diego, CA) using the NextSeq 500/550 High Output Kit v2 (Illumina, San Diego, CA) according to the manufacturer's instructions. Sequenced raw data was loaded onto BaseSpace

(Illumina, San Diego, CA) for subsequent data processing.

### Bioinformatics and biostatistics

Sequence reads were trimmed to remove sequencing adapters and low-quality bases, using Cutadapt v.1.10 (11). Data was then mapped against the Ensembl human reference genome (build GRCh38) with miRNA coordinates taken from miRBase v.21 (<http://www.mirbase.org>). Alignment and quantification steps were performed using Subread (<http://subread.sourceforge.net/>) and Rsubread (<https://bioconductor.org/packages/release/bioc/html/Rsubread.html>), respectively.

Differential mRNA and miRNA expression analysis was performed using a quasi-likelihood F-test, adjusted for baseline differences between two technical replicates for each skin explant. Raw *p*-values were corrected for multiple testing using the Benjamini-Hochberg method. A false discovery rate (FDR)-adjusted *p*-value <0.05 was used as the cut-off.

### RT-qPCR

cDNA was reverse transcribed from 150 ng of purified RNA using High-Capacity cDNA Reverse Transcription Kit (Applied Biosystems, USA), according to the manufacturer's instructions. Real-time PCR was performed in duplicate for each gene on a QuantStudio 5 Real-Time PCR System (Applied Biosystems, USA) using TaqMan® Universal PCR Kit (Applied Biosystems, USA) and commercially available TaqMan® primers/probes (Supplementary Table S8). The *18S* gene was used to normalize expression data using the 2<sup>-ΔΔCt</sup> method. Normalized expression data was represented as a fold change (FC) and differences determined using a *t*-test. A *p*-value <0.05 was considered significant.

### Gene annotation

PANTHER (Protein ANALYSIS THrough Evolutionary Relationships) Gene List Analysis (<http://pantherdb.org/>) was used to classify genes according to Molecular Function, Biological Process, Cellular Component, Protein Class and Pathway (12).

Tissue expression data provided by The Human Protein Atlas (<https://www.proteinatlas.org/>) was used to identify the skin cell types the DEGs were expressed in (13,14).

### KEGG pathway enrichment analysis

KEGG (Kyoto Encyclopedia of Genes and Genomes) pathway analysis of DEGs was performed using Web-based Gene Set Analysis Toolkit (WebGestalt) (<http://www.webgestalt.org>) (15). Human protein-coding genes were used as the reference dataset with the minimum number of genes for enrichment set at 5 and the FDR at <0.05.

### miRNA-target gene analysis

MiRNA-target gene interactions were determined using target prediction algorithms from miRDB (16), TargetScanHuman 7.2 (17), DIANA-microT-CDS (18), and miRWalk (19). Candidate targets found in at least 3 target prediction databases were considered valid. Additionally, we included all experimentally validated targets deposited in miRTarBase (20) and miRSearch

(<https://www.exiqon.com/miRSearch>). MiRNA-target gene networks were constructed considering that mRNA and miRNA expression levels should be inversely correlated if one regulates the other.

### HIF-1 $\alpha$ immunostaining

5  $\mu$ m skin sections were immunostained with an anti-HIF-1 $\alpha$  antibody (Novus Biologicals, Centennial, CO) overnight at 4°C. Samples were then incubated for 1h at room temperature with secondary antibody (Goat anti-Mouse IgG [Cy3]; Novus Biologicals, Centennial, CO). For all experimental conditions, a control without primary antibody was included.

### Image acquisition and analysis

Specimens were mounted with anti-fading medium (Fluoromount™, Sigma-Aldrich, St. Louis, MO) and imaged with a NanoZoomer S360 and NDP.view2 software (Hamamatsu Photonics, Hamamatsu City, Japan). Quantitative analysis was performed using Image J software (NIH, Bethesda, MD) by determining the Mean Grey Value of the area of the epidermis. 20 images/experimental condition were analyzed for each experimental condition. Statistical analysis was performed using Tukey's multiple comparison test. A *p*-value <0.05 was considered significant.

### Ethical approval and informed consent

All human skin explants used in this study were obtained with informed consent under authorization granted by the French government ethical committee according to French law L.1245 CSP.

## Results

### Gene expression analysis following anti-aging treatment

Expression of 168 genes (96 upregulated and 72 downregulated) was modified upon 3-in-1 NFS treatment, compared to 110 for ATIP, 7 each for melatonin and bakuchiol, and 6 for the vehicle alone (Table 1 and Supplementary Table S1). Notably, 75% (126) of these genes were uniquely modulated by 3-in-1 NFS (74 upregulated and 52 downregulated).

In order to validate the expression data from our RNA-Seq analysis, 13 genes were selected for further gene expression analysis using TaqMan®-based quantitative RT-PCR (RT-qPCR). Good reproducibility was observed between the two platforms (*p* = 0.58; Supplementary Figure S1), confirming the validity of the RNA-Seq data.

Many of the genes upregulated by 3-in-1 NFS have previously been shown to play important roles in skin biology (Table 2), including genes involved in collagen

synthesis (i.e., *P4HA1*), formation of the cornified cell layer responsible for barrier function (e.g., *SPRR2A*), and protection of the epidermis against UVB irradiation (i.e., *BNIP3*) (21–24). Other genes involved in angiogenesis (e.g., *VEGFA*) and glucose metabolism (e.g., *LDHA*), both processes compromised in photoaged skin (25–27), were also upregulated.

Amongst the downregulated genes, many were involved in immune- and inflammatory-related processes (Table 2), including cytokines (i.e., *CXCL14*), cytokine receptors (i.e., *CSF1R*), chemokines (e.g., *CCL2*), and chemokine receptors (i.e., *CCR2*). Other genes implicated in antigen processing (i.e., *ERAP2*), antigen presentation (e.g., *CD1A*), and complement activation (i.e., *C1S*), were also downregulated. Expression of enzymes involved in ROS detoxification (i.e., *GPX2*) and removal of toxic end products of lipid peroxidation (i.e., *ALDH3A*) were also decreased.

Based upon protein expression data provided in The Human Protein Atlas, keratinocytes were predicted to be the principle cell type affected by topical 3-in-1 NFS treatment (Supplementary Figure S2 and Supplemen-

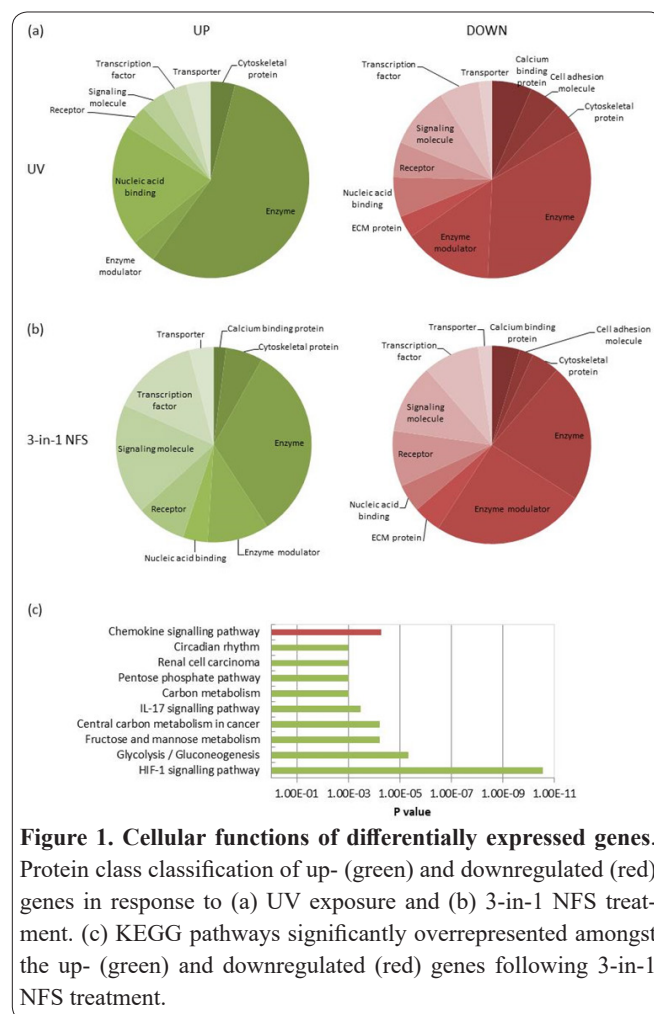


**Figure 1. Cellular functions of differentially expressed genes.** Protein class classification of up- (green) and downregulated (red) genes in response to (a) UV exposure and (b) 3-in-1 NFS treatment. (c) KEGG pathways significantly overrepresented amongst the up- (green) and downregulated (red) genes following 3-in-1 NFS treatment.

**Table 1.** Number of differentially expressed mRNAs and miRNAs following anti-aging treatment.

Regulation		3-in-1 NFS	Melatonin	Bakuchiol	ATIP	Vehicle
UP	mRNA	96	2	7	40	2
	miRNA	5	4	2	10	17
DOWN	mRNA	72	5	0	70	4
	miRNA	30	3	13	20	27
TOTAL	mRNA	168	7	7	110	6
	miRNA	35	7	15	30	44

**Table 2.** Biological functions of key genes differentially regulated by 3-in-1 NFS.

Regulation	Role	Gene	Description	Fold change		
UP	Collagen synthesis	<i>P4HA1</i>	prolyl 4-hydroxylase subunit alpha 1	2.81		
	Angiogenesis	<i>VEGFA</i>	vascular endothelial growth factor A	3.32 <sup>a</sup>		
UP	Glucose metabolism	<i>PGF</i>	placental growth factor	2.89		
		<i>ENO2</i>	enolase 2	5.03		
		<i>PFKFB3</i>	6-phosphofructo-2-kinase/fructose-2,6-biphosphatase 3	4.99		
		<i>SLC2A3</i>	solute carrier family 2 member 3	4.03		
		<i>PPP1R3C</i>	protein phosphatase 1 regulatory subunit 3C	3.43		
		<i>HK2</i>	hexokinase 2	2.93		
		<i>SLC2A1</i>	solute carrier family 2 member 1	2.60		
		<i>PDK1</i>	pyruvate dehydrogenase kinase 1	2.41		
		<i>PFKP</i>	phosphofructokinase, platelet	2.19		
		<i>ALDOA</i>	aldolase, fructose-bisphosphate A	1.99		
		<i>GPI</i>	glucose-6-phosphate isomerase	1.82		
		<i>LDHA</i>	lactate dehydrogenase A	1.67		
		UP	Epidermal homeostasis	<i>SPRR2A</i>	small proline rich protein 2A	6.92 <sup>b</sup>
				<i>SPRR2B</i>	small proline rich protein 2B	3.63
<i>IGFBP3</i>	insulin like growth factor binding protein 3			3.63		
<i>SPRR2D</i>	small proline rich protein 2D			2.43		
<i>ANGPTL4</i>	angiopoietin like 4			2.14		
<i>EPHA2</i>	EPH receptor A2			1.77		
UP	Stress response	<i>DDIT4</i>	DNA damage inducible transcript 4	3.94 <sup>a</sup>		
		<i>GADD45B</i>	growth arrest and DNA damage inducible beta	3.41		
		<i>NDRG1</i>	N-myc downstream regulated 1	2.77		
UP	Inflammatory response	<i>CCL22</i>	C-C motif chemokine ligand 22	4.29 <sup>b</sup>		
		<i>CCL20</i>	C-C motif chemokine ligand 20	3.53 <sup>a</sup>		
		<i>IL36G</i>	interleukin 36 gamma	2.60		
		<i>AKIRIN2</i>	akirin 2	2.14		
UP	NF-κB signaling	<i>NFKBIA</i>	NFKB inhibitor alpha	1.78		
		<i>TRAF3IP2</i>	TRAF3 interacting protein 2	1.74		
UP	HIF-1 signaling	<i>EGLN3</i>	egl-9 family hypoxia inducible factor 3	2.19		
		<i>EGLN1</i>	egl-9 family hypoxia inducible factor 1	2.11		
UP	Retinoid signaling	<i>GPRC5C</i>	G protein-coupled receptor class C group 5 member C	2.08		
UP	Wnt signaling	<i>FZD10</i>	frizzled class receptor 10	2.55 <sup>a</sup>		
		<i>CSRNP1</i>	cysteine and serine rich nuclear protein 1	2.28		
UP	Transcription factors	<i>ATF3</i>	activating transcription factor 3	4.14 <sup>a</sup>		
		<i>PHLDA1</i>	plekstrin homology like domain family A member 1	2.68 <sup>a</sup>		
		<i>FHL2</i>	four and a half LIM domains 2	1.92		
		<i>TSC22D1</i>	TSC22 domain family member 1	1.92		
		<i>FOS</i>	Fos proto-oncogene, AP-1 transcription factor subunit	1.89 <sup>c</sup>		
UP	Apoptosis	<i>BNIP3</i>	BCL2 interacting protein 3	4.44		
		<i>DNASE1L3</i>	deoxyribonuclease 1 like 3	3.05		
		<i>BNIP3L</i>	BCL2 interacting protein 3 like	1.85		
		<i>FAM162A</i>	family with sequence similarity 162 member A	1.83		
UP	Circadian rhythm	<i>CIART</i>	circadian associated repressor of transcription	3.58		
		<i>NR1D1</i>	nuclear receptor subfamily 1 group D member 1	2.85 <sup>a</sup>		
		<i>PER1</i>	period circadian regulator 1	2.17		
		<i>BHLHE40</i>	basic helix-loop-helix family member e40	2.03		
UP	Lipid metabolism	<i>HILPDA</i>	hypoxia inducible lipid droplet associated	5.50 <sup>a</sup>		
		<i>PLIN2</i>	perilipin 2	4.29 <sup>a</sup>		
		<i>AADAC</i>	arylacetamide deacetylase	3.27		
		<i>ALOX15B</i>	arachidonate 15-lipoxygenase type B	2.64 <sup>a</sup>		
UP	Complement pathway	<i>CD55</i>	CD55 molecule (Cromer blood group)	1.82 <sup>a</sup>		

DOWN	Apoptosis	<i>XAF1</i>	XIAP associated factor 1	-8.33		
	DNA repair	<i>PARP1</i>	poly(ADP-ribose) polymerase 1	-1.92		
ECM organization		<i>PARP9</i>	poly(ADP-ribose) polymerase family member 9	-2.27		
		<i>DAG1</i>	dystroglycan 1	-1.72		
		<i>LAMB1</i>	laminin subunit beta 1	-1.79		
		<i>LAMB4</i>	laminin subunit beta 4	-2.22		
		<i>DCN</i>	decorin	-2.44		
		<i>LAMA4</i>	laminin subunit alpha 4	-4.76		
		Epidermal homeostasis		<i>LCE1E</i>	late cornified envelope 1E	-2.44 <sup>d</sup>
<i>S100B</i>	S100 calcium binding protein B			-3.23		
<i>FLG2</i>	filaggrin family member 2			-3.33		
<i>TP73</i>	tumor protein p73			-4.55		
<i>LCE5A</i>	late cornified envelope 5A			-5.00		
<i>BTC</i>	betacellulin			-7.69		
Inflammation/Immunity				<i>CXCL14</i>	C-X-C motif chemokine ligand 14	-2.17 <sup>d</sup>
		<i>ERAP2</i>	endoplasmic reticulum aminopeptidase 2	-2.27		
		<i>CSF1R</i>	colony stimulating factor 1 receptor	-2.56		
		<i>CCL2</i>	C-C motif chemokine ligand 2	-2.70		
		<i>LSP1</i>	lymphocyte specific protein 1	-3.03		
		<i>CCR2</i>	C-C motif chemokine receptor 2	-3.33		
		<i>HCK</i>	HCK proto-oncogene, Src family tyrosine kinase	-3.45 <sup>d</sup>		
		<i>IL37</i>	interleukin 37	-3.57		
		<i>FCER1A</i>	Fc fragment of IgE receptor 1a	-3.70		
		<i>CD1A</i>	CD1a molecule	-4.17		
		<i>IL1F10</i>	interleukin 1 family member 10	-5.26		
		<i>CCL5</i>	C-C motif chemokine ligand 5	-7.14 <sup>e</sup>		
		<i>CYBB</i>	cytochrome b-245 beta chain	-7.14		
		<i>IFIT1</i>	interferon induced protein with tetratricopeptide repeats 1	-20.0 <sup>d</sup>		
		Complement pathway	<i>C1S</i>	complement C1s	-1.96 <sup>d</sup>	
		Wnt signaling		<i>KCTD1</i>	potassium channel tetramerization domain containing 1	-2.08
				<i>APCDD1</i>	APC down-regulated 1	-2.50 <sup>d</sup>
Oxidative stress		<i>GPX2</i>	glutathione peroxidase 2	-2.70 <sup>d</sup>		
		<i>ALDH3A1</i>	aldehyde dehydrogenase 3 family member A1	-2.77 <sup>d</sup>		
Redox metabolism	<i>NADSYN1</i>	NAD synthetase 1	-1.69			
Cell cycle	<i>CCND1</i>	cyclin D1	-2.08			

<sup>a</sup> Also upregulated by ATIP; <sup>b</sup> also upregulated by bakuchiol; <sup>c</sup> downregulated by vehicle; <sup>d</sup> also downregulated by ATIP; <sup>e</sup> also downregulated by ATIP, melatonin and vehicle.

tary Tables S2a and S2b). However, other important skin resident cell types were also affected, including fibroblasts (e.g. *DCN*), melanocytes (e.g., *PREX1*), and Langerhans cells (e.g., *S100B*).

### Functional classification of DEGs

To gain further insight into the biological relevance of DEGs modulated by 3-in-1 NFS, up- and downregulated genes were functionally classified using the PANTHER classification system (Supplementary Tables S3a-S3e). For 3-in-1 NFS, “transcription factors” (7 genes) and “signaling molecules” (9 genes) were the principle protein classes upregulated upon 3-in-1 NFS treatment (Figure 1b). In contrast, these classes were more common amongst genes downregulated by UV (14 and 9 genes, respectively) (Figure 1a).

### Pathway enrichment analysis of treated explants

We next performed KEGG pathway enrichment analysis to identify biological pathways statistically over-

represented by 3-in-1 NFS DEGs. Upregulated genes were significantly enriched in pathways involving Hypoxia-Inducible Factor (HIF)-1 signaling, carbohydrate metabolism, interleukin (IL)-17 signaling and circadian rhythm signaling (Figure 1c and Supplementary Table S4a). Downregulated genes were significantly enriched in pathways involved in cytokine signaling (Figure 1c and Supplementary Table S4b).

### 3-in-1 NFS modulates miRNA expression

Given its impact on gene expression, we hypothesized 3-in-1 NFS might also modulate microRNA (miRNA) expression levels. MiRNAs are short non-coding RNAs that regulate gene expression by hybridizing to complementary *cis*-regulatory elements in target mRNAs, resulting in their degradation or translational repression (28). To identify differentially expressed miRNAs following 3-in-1 NFS treatment, we performed a comparative miRNA expression profiling analysis. Thirty-five miRNAs (30 downregulated and 5

upregulated) were found to be differentially expressed following 3-in-1 NFS treatment (Table 1 and Supplementary Table S5).

### Integrative analysis of miRNA and mRNA expression profiles

To understand the miRNA regulatory networks modulated upon 3-in-1 NFS treatment, we predicted miRNA-target relationships in our dataset of 168 DEGs and established a mRNA-miRNA interactome. Network analysis identified 158 regulations (16 up- and 142 downregulated) between 35 miRNAs (30 down- and 5 upregulated) and 75 target genes (63 up- and 12 downregulated), accounting for 44.6% (75 of 168) of the total gene expression changes observed. Based on this, we performed KEGG pathway enrichment analysis for these 75 target genes. Amongst this gene set, only HIF-1 signaling was significantly enriched (Supplementary Table S6).

### 3-in-1 NFS specifically downregulates HIF-1-associated miRNAs

We next sought to understand which genes are specifically regulated by the miRNAs modulated exclusively by 3-in-1 NFS. We therefore established miRNA-target gene regulatory relationships for this subset of 16 miRNAs. Based on these relationships, our analysis predicted that these 3-in-1 NFS-specific miRNAs accounted for 60 regulations between 12 miRNAs (no regulations were predicted for let-7i-3p, miR-487b-3p, miR-7641 and miR-184) and 40 genes. Notably, half of these genes ( $n=20$ ) were predicted to be transcriptionally activated by HIF-1 (Supplementary Figure S3).

### Effect of 3-in-1 NFS on HIF-1 expression

Considering our RNA-Seq and miRNA expression data suggested that HIF-1 may be central to the biological activity of 3-in-1 NFS, we sought to examine HIF-1 expression in our explant samples. HIF-1 is a heterodimeric transcription factor comprising a constitutively expressed  $\beta$ -subunit and an oxygen-regulated  $\alpha$ -subunit (29,30). In skin, HIF-1 $\alpha$  is expressed in the basal and suprabasal layers of the epidermis where it is believed to play an important role in local and systemic adaptation to environmental stresses (31,32). Chronic UVB irradiation, however, suppresses HIF-1 $\alpha$  protein expression (33,34). In agreement with this, HIF-1 $\alpha$  protein levels in our UV-exposed skin explants were 45% lower than those in unexposed explants ( $p<0.0001$ ) (Figure 2b). Treatment with 3-in-1 NFS following UV exposure, however, significantly increased HIF-1 $\alpha$  levels by 42% ( $p<0.0001$ ), and levels approached those of unexposed control skin (Figure 2b). HIF-1 $\alpha$  mRNA levels were also higher (1.33-fold,  $p =$  not significant; Figure 2c). Notably, the vehicle alone had no effect on either HIF-1 $\alpha$  mRNA or protein levels (Figure 2b and Figure 2c). Together these data suggest that treatment with 3-in-1 NFS partially restores HIF-1 $\alpha$  protein expression in the epidermis of photoaged skin by modulating HIF-1 $\alpha$  mRNA and protein turnover.

### Discussion

3-in-1 NFS was specifically designed to address con-

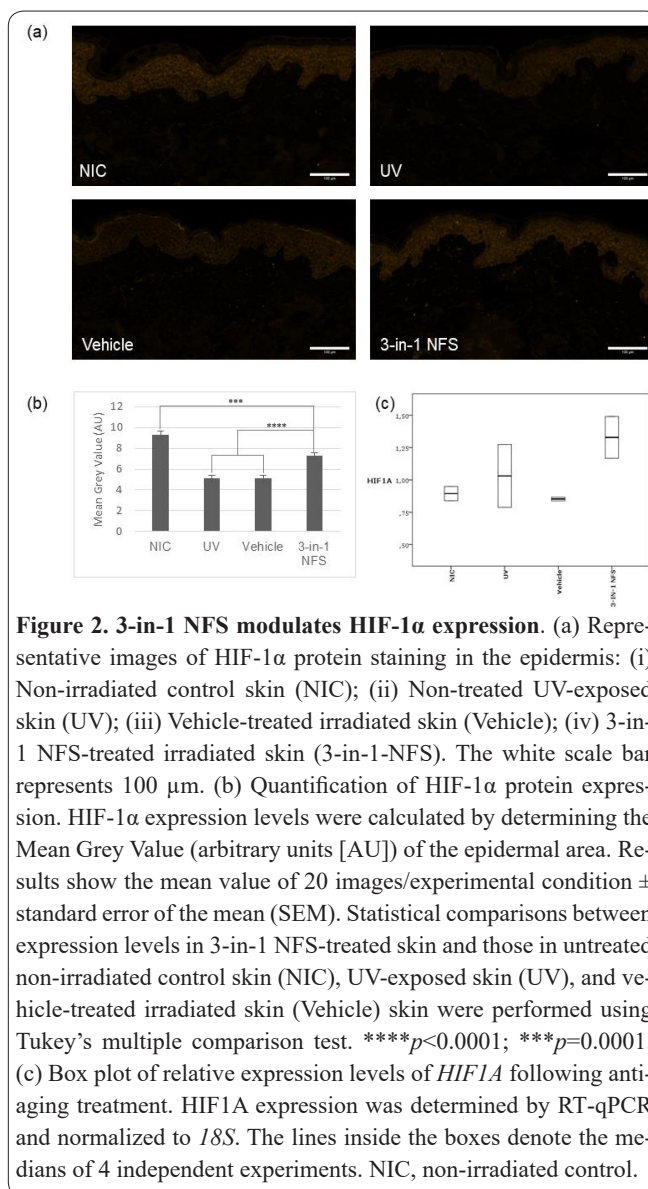


**Figure 2. 3-in-1 NFS modulates HIF-1 $\alpha$  expression.** (a) Representative images of HIF-1 $\alpha$  protein staining in the epidermis: (i) Non-irradiated control skin (NIC); (ii) Non-treated UV-exposed skin (UV); (iii) Vehicle-treated irradiated skin (Vehicle); (iv) 3-in-1 NFS-treated irradiated skin (3-in-1-NFS). The white scale bar represents 100  $\mu$ m. (b) Quantification of HIF-1 $\alpha$  protein expression. HIF-1 $\alpha$  expression levels were calculated by determining the Mean Grey Value (arbitrary units [AU]) of the epidermal area. Results show the mean value of 20 images/experimental condition  $\pm$  standard error of the mean (SEM). Statistical comparisons between expression levels in 3-in-1 NFS-treated skin and those in untreated non-irradiated control skin (NIC), UV-exposed skin (UV), and vehicle-treated irradiated skin (Vehicle) skin were performed using Tukey's multiple comparison test. \*\*\*\* $p<0.0001$ ; \*\*\* $p=0.0001$ . (c) Box plot of relative expression levels of *HIF1A* following anti-aging treatment. HIF1A expression was determined by RT-qPCR and normalized to *18S*. The lines inside the boxes denote the medians of 4 independent experiments. NIC, non-irradiated control.

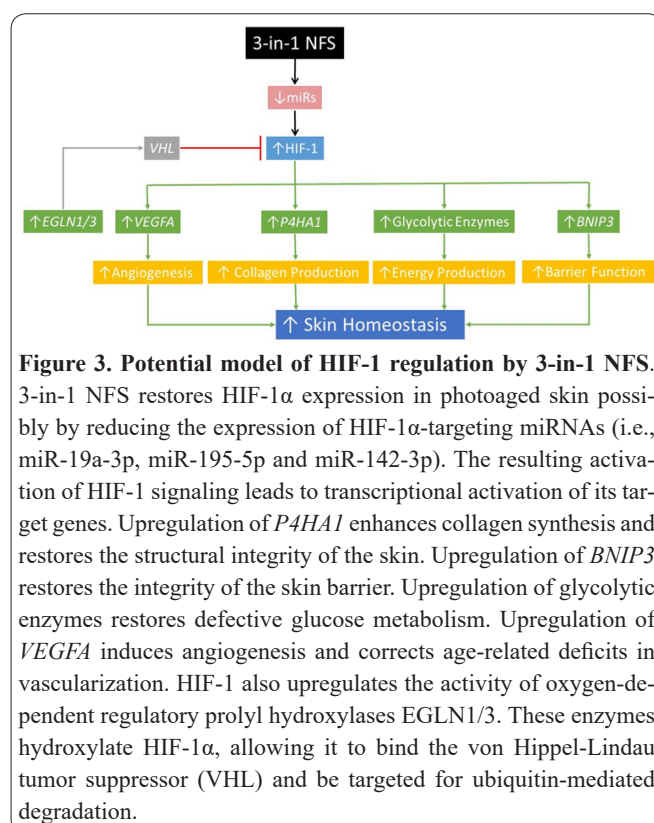


**Figure 3. Potential model of HIF-1 regulation by 3-in-1 NFS.** 3-in-1 NFS restores HIF-1 $\alpha$  expression in photoaged skin possibly by reducing the expression of HIF-1 $\alpha$ -targeting miRNAs (i.e., miR-19a-3p, miR-195-5p and miR-142-3p). The resulting activation of HIF-1 signaling leads to transcriptional activation of its target genes. Upregulation of *P4HA1* enhances collagen synthesis and restores the structural integrity of the skin. Upregulation of *BNIP3* restores the integrity of the skin barrier. Upregulation of glycolytic enzymes restores defective glucose metabolism. Upregulation of *VEGFA* induces angiogenesis and corrects age-related deficits in vascularization. HIF-1 also upregulates the activity of oxygen-dependent regulatory prolyl hydroxylases EGLN1/3. These enzymes hydroxylate HIF-1 $\alpha$ , allowing it to bind the von Hippel-Lindau tumor suppressor (VHL) and be targeted for ubiquitin-mediated degradation.

sumer demand for a product that could safely and effectively improve the appearance of photoaged skin. The results of this study in *ex vivo* human skin suggest that some of the biological events underpinning it might be mitigated by topical application of 3-in-1 NFS.

Remarkably, the combination of active ingredients in 3-in-1 NFS induced far more gene expression changes in our skin model following chronic UV exposure than any one of its individual components. In fact, 75% of the gene expression changes induced by 3-in-1 NFS were unique to it, suggesting that the combination of melatonin, bakuchiol and ATIP exerts a synergistic effect on gene expression. Antioxidant synergism between melatonin and vitamin C has previously been reported, with melatonin thought to reverse the pro-oxidant activity of vitamin C (35), however further studies are warranted to better understand the synergistic effect of melatonin, bakuchiol and ATIP in 3-in-1 NFS. The limited effect of melatonin and bakuchiol in isolation was equally surprising, each modulating only 7 genes (Table 1). A previous transcriptomic analysis of bakuchiol in skin saw hundreds of genes affected (7). This difference is most probably related to individual experimental design, although it cannot be ruled out that our results are an individual effect related to the particular donor skin used in our study. Therefore, additional studies on a larger number of skin explants, including unirradiated skin, should be performed. Likewise, histological studies on photoaged skin biopsies are warranted.

Seven of the miRNAs downregulated by 3-in-1 NFS (miR-382-5p, miR-143-3p, miR-132-3p, miR-126-3p, miR-145-5p, miR-30a-5p, and miR-21-5p) had previously been shown to be upregulated in sun-exposed skin (36). Amongst these, miR-145-5p was identified as a core miRNA reflecting the overall impact of sun exposure (36). Modulation of this miRNA is particularly significant as it targets genes implicated in some of the fundamental cellular signaling pathways regulating epidermal development and skin homeostasis, including barrier function (tight junctions signaling), collagen production (transforming growth factor [TGF]  $\beta$  signaling), and angiogenesis (vascular endothelial growth factor [VEGF] signaling) (36). Notably, we see upregulation of genes involved in all of these processes following 3-in-1 NFS treatment: *P4HA1* and *VEGFA*, which are both targets of miR-145-5p, encode key proteins involved in collagen biosynthesis and angiogenesis, respectively (21,26); and *EPHA2*, encodes a receptor tyrosine kinase that regulates epidermal tight junction formation (37).

Our transcriptomic data also provide compelling evidence that 3-in-1 NFS restores HIF-1 signaling in UV-exposed skin. Indeed, almost half (43 of 96) of the genes upregulated by 3-in-1 NFS are known HIF-1 target genes, many of which play important roles in maintaining skin physiology (Supplementary Table S7). It has previously been shown that that loss of HIF-1 accelerates epidermal aging and its restoration can reverse age-related impairment of the skin (38,39). Thus a well-tolerated cosmetic that restores HIF-1 activity and the expression of its target genes would be of particular benefit to photoaged skin and potentially mitigate some of the biological events responsible for it. Moreover, since HIF-1 is known to play important roles in cutane-

ous wound healing (40) and nociception (41), the combination of melatonin, bakuchiol and ATIP may have application to skin beyond photoaging.

To our knowledge, 3-in-1 NFS is the first non-drug demonstrated to act upon HIF-1 in the skin. This finding is all the more remarkable considering melatonin, bakuchiol and vitamin C in isolation have been shown to have the opposite effect on HIF-1 $\alpha$  levels (42–44). How then 3-in-1 NFS increases HIF-1 $\alpha$  mRNA and protein expression remains to be established and additional studies are warranted to better understand this apparent paradox. Our miRNA interactome analysis, however, eludes to a potential role for one or more of the 16 miRNAs uniquely downregulated upon 3-in-1 NFS treatment (Supplementary Figure S2). Amongst these, miR-19a-3p has been shown to affect HIF-1 $\alpha$  independently of hypoxia (45), and miR-195-5p and miR-142-3p to target HIF-1 $\alpha$  directly (46–48). As such, repression of their expression upon 3-in-1 NFS treatment could account for the higher HIF-1 $\alpha$  mRNA and protein levels we observed. Future studies may help clarify this.

In summary, we show that 3-in-1 NFS modulates the expression of numerous genes that might help attenuate some of the biological processes underpinning skin photoaging. Our transcriptomic analysis suggests that this is principally driven by HIF-1 $\alpha$  that is partially restored upon 3-in-1 NFS treatment. This increase in HIF-1 $\alpha$ , in turn, drives the expression of genes that may positively influence skin homeostasis (Figure 3).

## Acknowledgements

The authors wish to thank Jessica Romero, Claudia Navarro and Anna Rodriguez of Leitat who performed the HIF-1 $\alpha$  staining; Ursula Estada of the Multigenic Analysis Unit from UCIM-INCLIVA who helped perform the RNA-Seq and small-RNA-Seq experiments; and Daymé González of Bioinformatics Unit from EpiDisease S.L., who assisted with the bioinformatic analysis. Thanks also to Carles Trullas of ISDIN for his helpful comments on the manuscript.

## Interest conflict

MN and CG are employees of ISDIN, the manufacturer of 3-in-1 NFS. AB is a paid consultant to ISDIN. DPC and JLGG were paid by ISDIN to conduct this study.

## Author's contribution

MN, CG and JLGG designed the study. JLGG and DPC performed the experiments. AB and DPC analyzed the data. AB wrote the paper.

## References

1. Rittie L, Fisher GJ. Natural and sun-induced aging of human skin. *Cold Spring Harb Perspect Med* 2015; 5: a015370.
2. Wang S, Zhu F. Dietary antioxidant synergy in chemical and biological systems. *Crit Rev Food Sci Nutr* 2017; 57: 2343–57.
3. Ochiai Y, Kaburagi S, Obayashi K, Ujiiie N, Hashimoto S, Okano, Y *et al.* A new lipophilic pro-vitamin C, tetra-isopalmitoyl ascorbic acid (VC-IP), prevents UV-induced skin pigmentation through its anti-oxidative properties. *J Dermatol Sci* 2006; 44: 37–44.
4. Maia Campos PMBG, Gianeti MD, Camargo FBJ, Gaspar LR. Application of tetra-isopalmitoyl ascorbic acid in cosmetic

formulations: stability studies and in vivo efficacy. *Eur J Pharm Biopharm* 2012; 82: 580–6.

5. Fischer TW, Kleszczynski K, Hardkop LH, Kruse N, Zillikens D. Melatonin enhances antioxidative enzyme gene expression (CAT, GPx, SOD), prevents their UVR-induced depletion, and protects against the formation of DNA damage (8-hydroxy-2'-deoxyguanosine) in ex vivo human skin. *J Pineal Res* 2013; 54: 303–12.

6. Tan D, Reiter RJ, Manchester LC, Yan M, El-Sawi M, Sainz RM *et al.* Chemical and physical properties and potential mechanisms: melatonin as a broad spectrum antioxidant and free radical scavenger. *Curr Top Med Chem* 2002; 2: 181–97.

7. Chaudhuri RK, Bojanowski K. Bakuchiol: a retinol-like functional compound revealed by gene expression profiling and clinically proven to have anti-aging effects. *Int J Cosmet Sci* 2014; 36: 221–30.

8. Shoji M, Arakaki Y, Esumi T, Kohnomi S, Yamamoto C, Suzuki Y *et al.* Bakuchiol Is a Phenolic Isoprenoid with Novel Enantiomer-selective Anti-influenza A Virus Activity Involving Nrf2 Activation. *J Biol Chem* 2015; 290: 28001–17.

9. Adhikari S, Joshi R, Patro BS, Ghanty TK, Chintalwar GJ, Sharma A *et al.* Antioxidant activity of bakuchiol: experimental evidences and theoretical treatments on the possible involvement of the terpenoid chain. *Chem Res Toxicol* 2003; 16: 1062–9.

10. Goldberg DJ, Robinson DM, Granger C. Clinical evidence of the efficacy and safety of a new 3-in-1 anti-aging topical night serum-in-oil containing melatonin, bakuchiol, and ascorbyl tetraisopalmitate: 103 females treated from 28 to 84 days. *J Cosmet Dermatol* 2019; 18: 806-14

11. Martin M. Cutadapt Removes Adapter Sequences From High-Throughput Sequencing Reads. *EMBnet.journal* 2011; 17: 10–12.

12. Mi H, Muruganujan A, Ebert D, Huang X, Thomas PD. PANTHER version 14: more genomes, a new PANTHER GO-slim and improvements in enrichment analysis tools. *Nucleic Acids Res* 2019; 47: D419–D426.

13. Uhlen M, Oksvold P, Fagerberg L, Lundberg E, Jonasson K, Forsberg M. *et al.* Towards a knowledge-based Human Protein Atlas. *Nat Biotechnol* 2010; 28: 1248–50.

14. Uhlen M, Fagerberg L, Hallstrom BM, Lindskog C, Oksvold P, Mardinoglu A *et al.* Proteomics. Tissue-based map of the human proteome. *Science* 2015; 347: 1260419.

15. Wang J, Vasaikar S, Shi Z, Greer M, Zhang B. WebGestalt 2017: a more comprehensive, powerful, flexible and interactive gene set enrichment analysis toolkit. *Nucleic Acids Res* 2017; 45: W130–W137.

16. Wong N, Wang X. miRDB: an online resource for microRNA target prediction and functional annotations. *Nucleic Acids Res* 2015; 43: D146-52.

17. Lewis BP, Burge CB, Bartel DP. Conserved seed pairing, often flanked by adenosines, indicates that thousands of human genes are microRNA targets. *Cell* 2005; 120: 15–20.

18. Paraskevopoulou MD, Georgakilas G, Kostoulas N, Vlachos IS, Vergoulis T, Reczko M *et al.* DIANA-microT web server v5.0: service integration into miRNA functional analysis workflows. *Nucleic Acids Res* 2013; 41: W169-73.

19. Sticht C, La Torre C De, Parveen A, Gretz N. miRWalk: An online resource for prediction of microRNA binding sites. *PLoS One* 2018; 13: e0206239.

20. Chou C-H, Shrestha S, Yang C-D, Chang N-W, Lin Y-L, Liao K-W *et al.* miRTarBase update 2018: a resource for experimentally validated microRNA-target interactions. *Nucleic Acids Res* 2018; 46: D296–D302.

21. Pihlajaniemi T, Myllyla R, Kivirikko KI. Prolyl 4-hydroxylase and its role in collagen synthesis. *J Hepatol* 1991; 13 Suppl 3: S2-7.

22. Cabral A, Voskamp P, Cleton-Jansen AM, South A, Nizetic D,

Backendorf C. Structural organization and regulation of the small proline-rich family of cornified envelope precursors suggest a role in adaptive barrier function. *J Biol Chem* 2001; 276: 19231–7.

23. Moriyama M, Moriyama H, Uda J, Matsuyama A, Osawa M, Hayakawa T. BNIP3 plays crucial roles in the differentiation and maintenance of epidermal keratinocytes. *J Invest Dermatol* 2014; 134: 1627–35.

24. Moriyama M, Moriyama H, Uda J, Kubo H, Nakajima Y, Goto A *et al.* BNIP3 upregulation via stimulation of ERK and JNK activity is required for the protection of keratinocytes from UVB-induced apoptosis. *Cell Death Dis* 2017; 8: e2576.

25. Chung JH, Yano K, Lee MK, Youn CS, Seo JY, Kim, KH *et al.* Differential effects of photoaging vs intrinsic aging on the vascularization of human skin. *Arch Dermatol* 2002; 138: 1437–42.

26. Chung JH, Eun HC. Angiogenesis in skin aging and photoaging. *J Dermatol* 2007; 34: 593–600.

27. Yan W, Zhang L-L, Yan L, Zhang F, Yin N-B, Lin H-B *et al.* Transcriptome analysis of skin photoaging in chinese females reveals the involvement of skin homeostasis and metabolic changes. *PLoS One* 2013; 8: e61946.

28. Filipowicz W, Bhattacharyya SN, Sonenberg N. Mechanisms of post-transcriptional regulation by microRNAs: are the answers in sight? *Nat Rev Genet* 2008; 9: 102–14.

29. Huang LE, Gu J, Schau M, Bunn HF. Regulation of hypoxia-inducible factor 1alpha is mediated by an O2-dependent degradation domain via the ubiquitin-proteasome pathway. *Proc Natl Acad Sci U S A* 1998; 95: 7987–92.

30. Wang GL, Jiang BH, Rue EA, Semenza, GL. Hypoxia-inducible factor 1 is a basic-helix-loop-helix-PAS heterodimer regulated by cellular O2 tension. *Proc Natl Acad Sci U S A* 1995; 92: 5510–4.

31. Rezvani HR, Ali N, Nissen LJ, Harfouche G, de Verneuil H, Taieb A *et al.* HIF-1alpha in epidermis: oxygen sensing, cutaneous angiogenesis, cancer, and non-cancer disorders. *J Invest Dermatol* 2011; 131: 1793–1805.

32. Seleit I, Bakry OA, Al-Sharaky DR, Ragab RAA, Al-Shiemy SA. Evaluation of Hypoxia Inducible Factor-1alpha and Glucose Transporter-1 Expression in Non Melanoma Skin Cancer: An Immunohistochemical Study. *J Clin Diagn Res* 2017; 11: EC09-EC16.

33. Cho Y-S, Kim C-H, Park J-W. Involvement of HIF-1alpha in UVB-induced epidermal hyperplasia. *Mol Cells* 2009; 28: 537–43.

34. Wunderlich L, Paragh G, Wikonkal NM, Banhegyi G, Karpati S, Mandl J. UVB induces a biphasic response of HIF-1alpha in cultured human keratinocytes. *Exp Dermatol* 2008; 17: 335–42.

35. Gitto E, Tan DX, Reiter RJ, Karbownik M, Manchester LC, Cuzzocrea S *et al.* Individual and synergistic antioxidative actions of melatonin: studies with vitamin E, vitamin C, glutathione and desferrioxamine (desferoxamine) in rat liver homogenates. *J Pharm Pharmacol* 2001; 53: 1393–1401.

36. Srivastava A, Karlsson M, Marionnet C, Bernerd F, Gueniche A, Rawadi CEL *et al.* Identification of chronological and photoageing-associated microRNAs in human skin. *Sci Rep* 2018; 8: 12990.

37. Perez White BE, Ventrella R, Kaplan N, Cable CJ, Thomas, PM, Getsios, S. EphA2 proteomics in human keratinocytes reveals a novel association with afadin and epidermal tight junctions. *J Cell Sci* 2017; 130: 111–8.

38. Rezvani HR, Ali N, Serrano-Sanchez M, Dubus P, Varon C, Ged C *et al.* Loss of epidermal hypoxia-inducible factor-1alpha accelerates epidermal aging and affects re-epithelialization in human and mouse. *J Cell Sci* 2011; 124: 4172–83.

39. Pagani A, Aitzetmuller MM, Brett EA, Konig V, Wenny R, Thor D. *et al.* Skin Rejuvenation through HIF-1alpha Modulation. *Plast Reconstr Surg* 2018; 141: 600e-607e.

40. Hong WX, Hu MS, Esquivel M, Liang GY, Rennert RC, McArdle

A *et al.* The Role of Hypoxia-Inducible Factor in Wound Healing. *Adv wound care* 2014; 3: 390–9.

41. Kanngiesser M, Mair N, Lim H-Y, Zschiebsch K, Bles J, Haussler A *et al.* Hypoxia-inducible factor 1 regulates heat and cold pain sensitivity and persistence. *Antioxid Redox Signal* 2014; 20: 2555–71.

42. Vissers MCM, Gunningham SP, Morrison MJ, Dachs GU, Currie MJ. Modulation of hypoxia-inducible factor-1 alpha in cultured primary cells by intracellular ascorbate. *Free Radic Biol Med* 2007; 42: 765–72.

43. Vriend J, Reiter R J. Melatonin and the von Hippel-Lindau/HIF-1 oxygen sensing mechanism: A review. *Biochim Biophys Acta* 2016; 1865: 176–83.

44. Wu C-Z, Hong SS, Cai XF, Dat NT, Nan J-X, Hwang, BY *et al.* Hypoxia-inducible factor-1 and nuclear factor-kappaB inhibitory

meroterpene analogues of bakuchiol, a constituent of the seeds of *Psoralea corylifolia*. *Bioorg Med Chem Lett* 2008; 18: 2619–23.

45. Loscalzo J. The cellular response to hypoxia: tuning the system with microRNAs. *J Clin Invest* 2010; 120: 3815–7.

46. Bai R, Zhao A-Q, Zhao Z-Q, Liu, W-L, Jian D-M. MicroRNA-195 induced apoptosis in hypoxic chondrocytes by targeting hypoxia-inducible factor 1 alpha. *Eur Rev Med Pharmacol Sci* 2015; 19: 545–51.

47. Tao B, Shi K. Decreased miR-195 Expression Protects Rats from Spinal Cord Injury Primarily by Targeting HIF-1alpha. *Ann Clin Lab Sci* 2016; 46: 49–53.

48. Lu Y, Ji N, Wei W, Sun W, Gong X, Wang X. MiR-142 modulates human pancreatic cancer proliferation and invasion by targeting hypoxia-inducible factor 1 (HIF-1alpha) in the tumor microenvironments. *Biol Open* 2017; 6: 252–9.